MODELING AND DYNAMIC ANALYSIS OF AEROSPACE VIBRATION ISOLATORS FOR VIBRATION TRANSMISSION CONTROL

Isabel Lima Hidalgo, isabel@embraer.com.br
Airton Nabarrete, nabarret@ita.br
Engenharia Aeronáutica – IEA
Instituto Tecnológico de Aeronáutica - ITA
Praça Mal.Eduardo Gomes 50 - Vila das Acácias
12228-900 - São José dos Campos - SP - Brasil

Marcelo Santos, marcelo.santos@embraer.com.br
Embraer S/A
Av. Brigadeiro Faria Lima, 2170
12227-901 - São José dos Campos - SP - Brasil

Abstract. *One of the existing challengers on the aircraft design is the cabin internal noise reduction. In this direction, this work emphasizes the transmission paths modeling taking into consideration vibration isolators for the structure-borne energy isolation between the fuselage and the aircraft interior. As a result of this transmissibility reduction, the vibration isolators play an important role in the interior noise control throughout an extensive frequency range. In general, simplified models are not able to predict the isolator performance at mid and high frequencies, since they do not take into account the isolator internal resonances. A finite element model is employed to assess a typical aeronautic isolator dynamic behavior. The identification of its material properties is carried out based on dynamic stiffness, which were verified through experimental frequency response analysis. After the model update, a dynamic analysis of the isolator applied between plates is performed via FEA. Different approaches and complexity of the isolator are modeled, resulting in distinct responses depending on the frequency of concern. In the high frequency range where the isolator modes are concentrated, the great number of plate modes cause difficulties in identifying the isolator internal dynamic influence in whole system response. The results interpretation at high frequency demonstrates the difficult of applying the finite element method, due to its deterministic and nodal response, since it point out the presence of local modes. In order to overcome this restriction, this work also makes a brief use of the Statistical Energy Analysis (SEA), jointly with the finite element method, helping on the identification of the real importance of the structure-borne path at high frequency.*

Keywords: *Vibration Isolators, Dynamic Analysis, FEA, SEA*

1. INTRODUCTION

Conceptually, according to Beranek (1992) vibration isolators are resilient elements placed between two structures aiming at minimizing the vibration transmission. As applications, isolators are applied for reduction of vibration transmission and noise radiation. In the aeronautic industry these applications are of great practical relevance, for instance the extensive use of vibration isolators between fuselage and interior panels. Due to this expressive presence, the proper representation of these isolators in computer models for interior noise prediction is of vital importance for the accurate evaluation of the vibration transmission paths between fuselage and the aircraft interior.

The vibration isolators made of elastomeric materials are the most commonly used, due to its propitious mechanical properties, such as high damping, low stiffness, and high bearing capacity (Downey *et al.* 2001). The correct material characterization plays an important role in the isolator performance evaluation. The elastomeric material is defined mainly by the application ambient conditions and load. The temperature is one of the most important parameter, since this material at low temperature tends to be stiffer and have higher damping, and at high temperatures tends to lose stiffness and damping. In addition, the elastomeric properties are strongly dependent on the frequency and strain (Jones, 2001). Some instances of elastomeric materials applied in the vibration control are natural rubber, neoprene, and silicone. This last one is largely used in aeronautics since it is recommended for broad temperatures range.

Different methods can be found to evaluate the isolator behavior. The classic method represents the system as a mass-spring-damper and is useful at low frequency (Nashif, 1985). Nevertheless, this representation does not include features of the real system, such as material non-linearities, isolator dynamic behavior, the fact of the isolated structure do not behave as a rigid body; which all influence the isolator attenuation at mid and high frequencies (Snowdon, 1979, Beranek, 1992; Weisbeck, 2006). On the other hand the Four-Pole method, described by Molloy (1957) incorporates the isolator and the structure dynamic characteristics through the frequency dependent transfer matrix. The Four-pole parameters are usually obtained experimentally (Snowdon, 1979, Weisbeck, 2006, Weisbeck *et al.*, 2009).

An alternative method to assess the isolator attenuation considering its dynamic behavior is through detailed models in finite element method (Jones, 2001). This is a robust and well-established method to solve engineering problems related to structure, fluid and solid (Bathe, 1996). In the discussed case this method is suitable, since a detailed isolator description is required regarding geometry, material properties, and dynamic behavior.

The current paper discusses the results of modeling an aircraft interior panel isolator as a solid finite element model (FEM). Some dynamic analyses are performed and the material properties of the model are updated by experimental data. Different approaches and complexities for the isolator models are investigated, resulting in distinct responses depending on the frequency of concern. Additionally, the use of the Statistical Energy Analysis (SEA) helps on the identification the real importance of the structure-borne path at high frequency.

2. ISOLATOR MODELING

2.1. Finite Element Model Description

An isolator component typically used for aircraft interior panels is modeled in this paper. Its catalog static stiffness is 88000 N/m (Lord Corporation, 2010). The basic dimensions are 8.25 mm of height, and 47 mm of width. The isolator finite element model depicted in Fig. 1(a) contains 9626 solid elements (HEXA and PENTA), and 11115 nodes. Three different materials properties are described in Tab. 1 and highlighted on Fig. 1(b). The dynamic analysis was performed employing a Nastran solver (MSC Software, 2008).

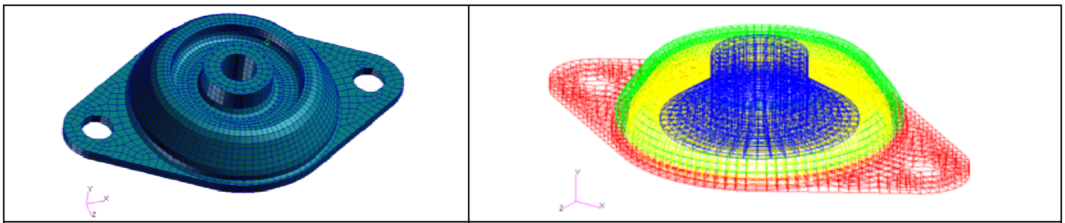

a. Isolator finite element mesh	b. Isolator materials: regions made of aluminum in red and green, elastomer in yellow and steel in blue.

Figure 1. Isolator finite element model.

Table 1. Isolator material properties

Isolator part	Material	Density $[kg/m^3]$	Poisson coefficient	Loss Factor	Young Modulus [Pa]
External structure	Aluminum	2700	0.33	1%	7.1×10^{11}
Central Fixture	Steel 304 SS	8300[1]	0.28	1%	2.0×10^{11}
Elastomer	Silicone	1200	0.40	20%	2.5×10^{6}

(1): density to updated isolator mass

Considering the finite elements present in the model, in order to correctly represent a mode of vibration, a minimum number of elements per wavelength is required. According to Fahy and Gardonio (2007) six elements per wavelength can be used as reference. The wavelength λ is described by the Eq. (1).

$$\lambda = c/f \tag{1}$$

In Eq. (1), c is the wave propagation speed, and f is the frequency. In this current case, c is the quasi-longitudinal wave speed in solids for a bar c_l presented in Eq. (2).

$$c_l = (E/\rho)^{1/2} \tag{2}$$

The model mesh is based on 0.7 mm elements. Considering the material properties described at Tab. 1, the lower wave speed occurs for the lower Young Modulus, given by the elastomeric material. The lower the wave speed the lower the mesh frequency limit. Hence, taking into account the elastomer properties and 10 elements per mode ($\lambda = 10.d = 7\ mm$), the frequency limit for the current mesh is approximately 6500 Hz.

2.2. Elastomeric material properties identification

The elastomeric material is of great importance for the isolator model response. At the same time, usually it is difficult to obtain this information from manufacturers. Therefore, in the present case, the identification of the elastomer properties was based on dynamic stiffness measurements and later numerical adjustment.

As a test procedure for axial dynamic stiffness measurement (Clark and Hain, 1996), the isolator was excited axially by a shaker at one end and the other was held fix; approximating the experiment to one-degree-of-freedom system. The resultant accelerance given by the ratio between acceleration $\ddot{x}$ and applied force F was taken. Disregarding the isolator mass, the dynamic stiffness k is calculated by the Eq. (3), where m is the mass supported by the isolator, which corresponds to the attachment apparatus such as bolts and washers; and f is the frequency in Hz.

$$k = \left(m - \frac{F}{\ddot{x}}\right)(2\pi f)^2 \tag{3}$$

The test result is presented on Fig. 2. The first peak is associated to test assembly. The test data are only considered valid where the dynamic stiffness is constant, which is below system resonance. Above this value the response is controlled by inertia, explaining the decrease in stiffness. From the test, the value for the dynamic stiffness real part is 1.5×10^5 N/m, and for the imaginary part is 2.9×10^4 N/m.

Afterwards, several frequency response analyses were performed using the isolator FE model in order to fit the experimental data. In this case, distinct values of elastomer Young modulus were considered, as present by material handbook (Material Data Base, 2010). The Young Modulus of 2.5 MPa and loss factor of 20%, resulted in the best dynamic stiffness curve adjustment, as can be verified in Fig. 2.

Frequency-constant properties were used for the isolator rubber material. Although the rubber properties are dependent on frequency, for typical applications of the isolator studied in the current work, it is possible to consider a constant Young Modulus value since the isolator elastomeric material is designed to work in the viscoelastic rubbery region.

In the finite element analysis FEA, a unitary axial concentrated force was applied on the isolator central fixture. No concentrated mass was considered, which differs from the experiment, and generate the later decreasing in real dynamic stiffness. In addition, no perturbation at low frequency is observed in the numerical analysis.

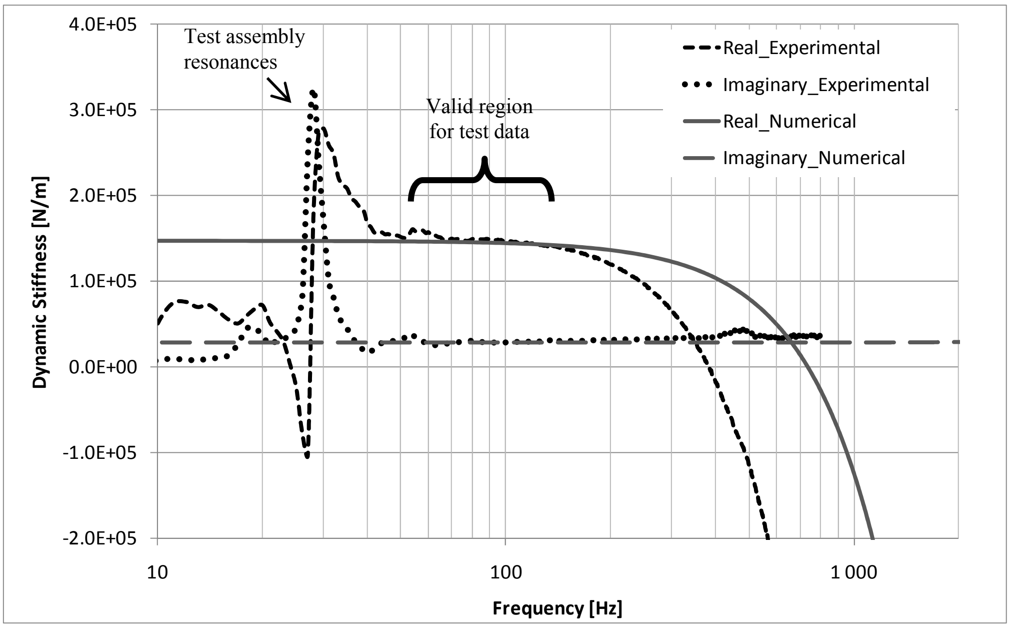

Figure 2: Dynamic Stiffness: comparison between numerical (FEM) and experimental, real and imaginary parts.

3. ISOLATOR DYNAMIC ANALYSIS

With the elastomeric material properties updated in the FE model, the isolator modal analysis was performed, in order to assess its dynamic behavior. The isolator is in a free-free condition; as a result the first six modes are rigid body modes and therefore are omitted of this analysis. The following six modes respond as springs, where the central fixture pin works as a concentrated mass and the elastomeric material as a spring element, being possible to visualize a six degree-of-freedom spring. As per Gardner *et al.* (2005), these modes are called spring modes; they are listed and depicted in Fig. 3. As a consequence of the geometry of this specific isolator, the radial modes are symmetric.

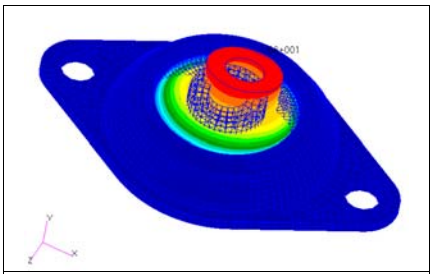
Mode 1. Radial mode 512.8 Hz

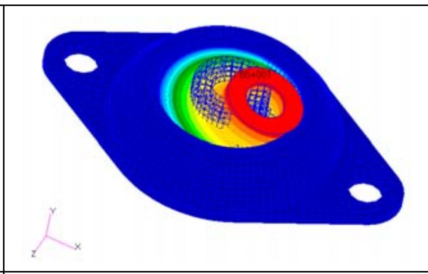
Mode 2. Radial mode 514.7 Hz

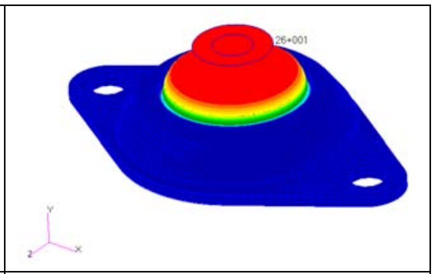
Mode 3. Axial mode 738.0 Hz

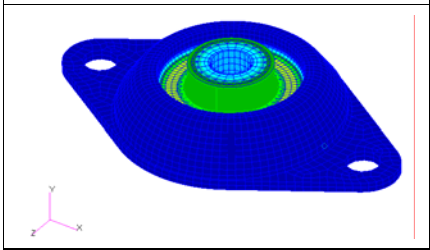
Mode 4. Torsion mode 755.3 Hz

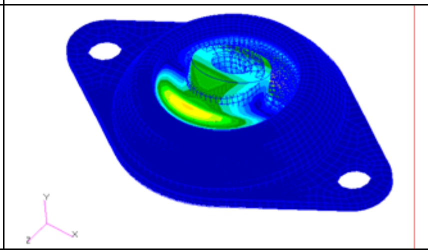
Mode 5. Rocking mode 1138.1 Hz

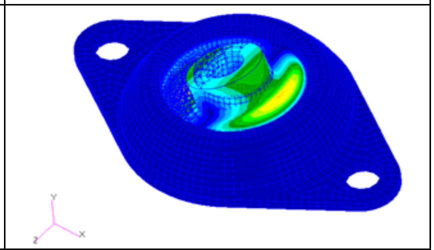
Mode 6. Rocking mode 1148.9 Hz

Figure 3. Isolator Spring Modes.

The modes following the spring modes are named the elastomeric material modes, in which only this more flexible part of the isolator responds; the external structure and the central fixture do not influence the isolator dynamic response. These elastomer modes concentrate at very high frequency, in the current case from 4000 Hz and on. They are symmetric and very close to each other in frequency. Table 2 describes the elastomer modes until 6500 Hz. Figure 4 shows some instances of elastomer mode shapes.

Table 2. Modes of the elastomeric material

Mode	Nat Freq [Hz]	Mode	Nat Freq [Hz]	Mode	Nat Freq [Hz]	Mode	Nat Freq [Hz]
7	4086.4	19	4804.9	31	5288.1	43	6091.9
8	4492.5	20	4804.9	32	5396.5	44	6096.2
9	4505.5	21	4813.8	33	5396.6	45	6104.9
10	4550.0	22	4814.8	34	5505.7	46	6104.9
11	4586.8	23	4931.5	35	5505.7	47	6240.9
12	4587.6	24	4931.5	36	5740.8	48	6240.9
13	4662.2	25	5053.3	37	5740.8	49	6275.2
14	4662.4	26	5053.5	38	5761.2	50	6275.4
15	4717.3	27	5060.7	39	5761.2	51	6403.9
16	4717.3	28	5094.5	40	5987.6	52	6403.9
17	4746.0	29	5094.5	41	5987.6	53	6496.7
18	4796.0	30	5288.1	42	6028.2	54	6496.7

4. FUSELAGE-ISOLATOR-INTERIOR AIRCRAFT PANEL

4.1. Finite Element Modeling

With the aim at evaluating approaches with different complexity for modeling isolators, one first model containing two flat plates centrally connected by an isolator is created. This model is aimed at recalling the concept of a fuselage-isolator-interior panel structure, being the isolator responsible for the attachment between parts and for the isolation of the fuselage vibration simultaneously.

Two identical plates of dimensions 0.5 m x 0.7 m, and thickness equal to 2 mm are modeled via FEA with QUAD4 elements. The plate material is aluminum, with the same properties described at Tab. 1. The plates are placed parallel with 8.25 mm of spacing, which correspond to the isolator height. The connection is made by the plate central points.

The rotation degree of-freedom on the plate edges direction was restricted with the aim of simulating the structure continuity.

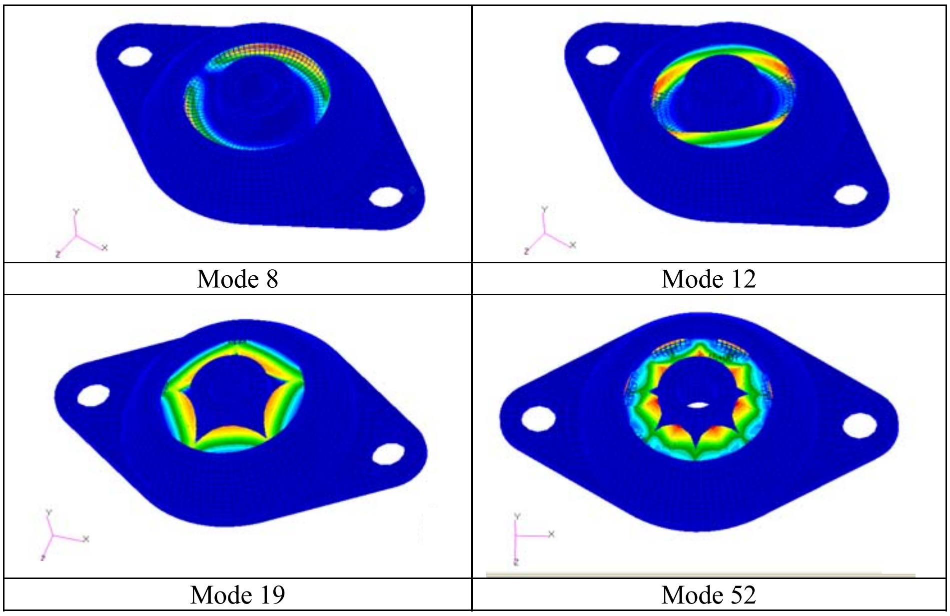

Figure 4. Instances of elastomeric material mode shapes.

Different approaches for modeling the isolators applied in the airplane fuselage are simulated. Modal frequency response analyses considering five distinct models to connect both plates in the central point are performed as follows:

1. Rigid connection: The isolator infinite stiffness is used only as reference to this simulation.
2. Linear axial spring with static stiffness of 88000 N/m obtained from catalog information.
3. Linear axial spring considering the constant dynamic stiffness value of 1.5 x 10^5 N/m, which is obtained from the axial direction test in the isolator experiment.
4. Six degree-of-freedom spring considering the values presented at Tab. 3. In this table, each value corresponds to a constant dynamic stiffness per direction. These constants are obtained from experiments similar to that described at section 2.2.
5. Updated FE solid model for the isolator as described in the previous sections.

Table 3. Constant dynamic stiffness values.

Direction	Dynamic Stiffness [N/m]	Loss Factor η
X	1.0E+05	0.18
Y	1.0E+05	0.18
Z	1.5E+05	0.20
θx	2.8E+01	0.20
θy	2.8E+01	0.20
θz	2.7E+01	0.14

In these analyses, the excitation force ranges from 1 to 8000 Hz. Initially only one concentrated harmonic force was applied perpendicular to the bottom plate. Subsequently it is proposed to create an average spectrum for each response. This is performed applying six different excitations arbitrarily distributed and applied not simultaneously, as shown sketched in Fig. 6.

Hence, the upper plate dynamic response is obtained averaging velocity in space considering nine chosen nodes, and afterward averaging these results for the six different excitations. This data is calculated for each model. Velocity magnitude is considered as the response parameter, since it characterizes the vibration level.

4.2. Results

The numerical analyses developed in this research evaluate the dynamic response of the upper plate when five different isolator models are applied as described above. In these simulations, the upper plate response is represented by the average value of nine points chosen on the plate area. The velocity magnitude is considered as response parameter, since it characterizes the vibration level.

Figure 5 brings the low frequency results (1 to 100 Hz) in narrow band. In this range, the six-DOF spring behavior was the closer to the isolator behavior. Significant differences among models must be noted in this figure, for instance the anti-resonance behavior when analyzing both axial spring models from 50 to 60 Hz, while the other models show a resonance at 60 Hz.

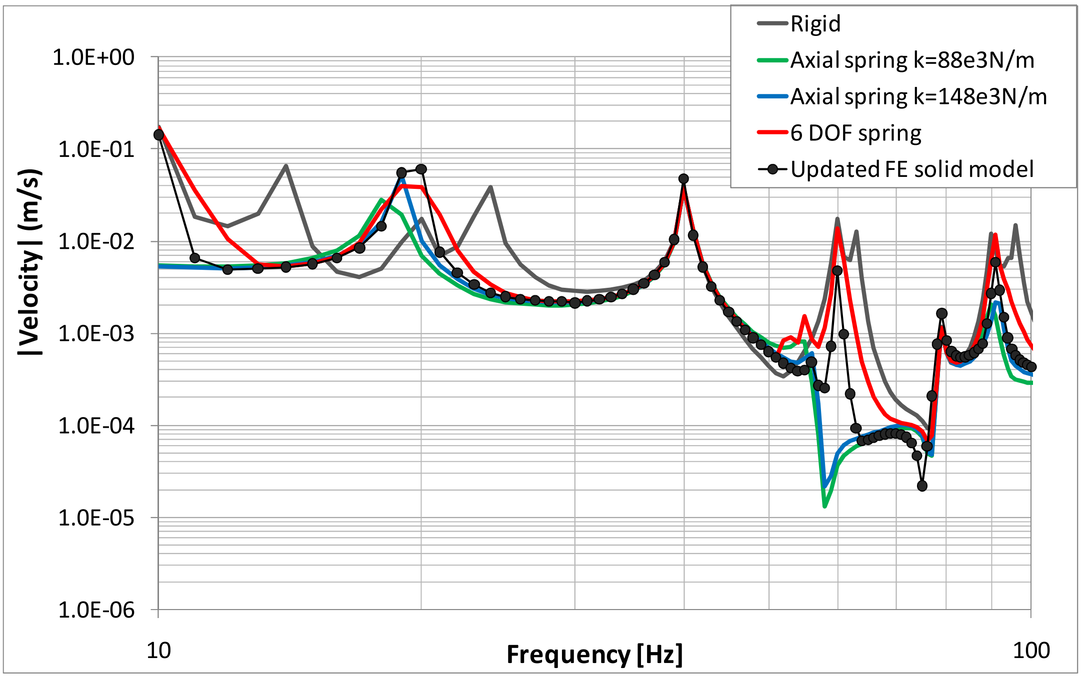

Figure 5. Upper plate velocity average in low frequency range (10 to 100 Hz).

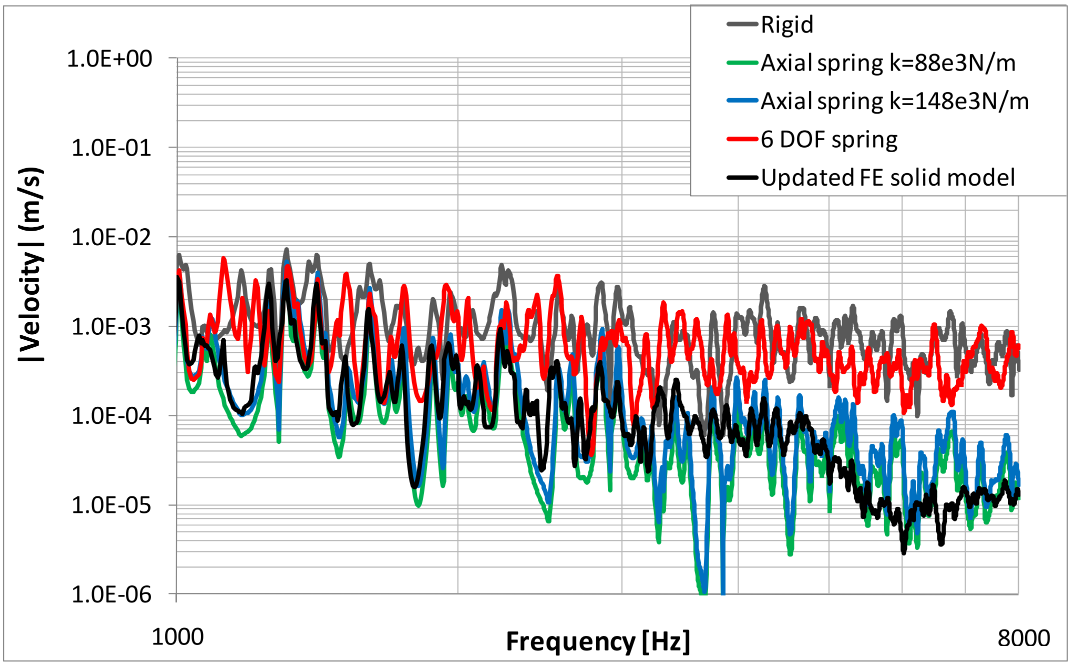

Figure 6. Upper plate velocity average in high frequency range (1000 to 8000 Hz).

Analyzing the isolator FE model result in Fig. 6, it is visible the large number of plate modes found in the same frequency range where the isolator internal modes (elastomeric material modes) are concentrated, i.e. above 4000 Hz. As a consequence, it is difficult to properly assess the influence of isolator internal resonances on the plate response.

Afterwards the average spectrum for each response are generated based on the response resulting from six different excitations as presented in Fig. 7 considering one-third octave frequency band from 100 to 6300 Hz.

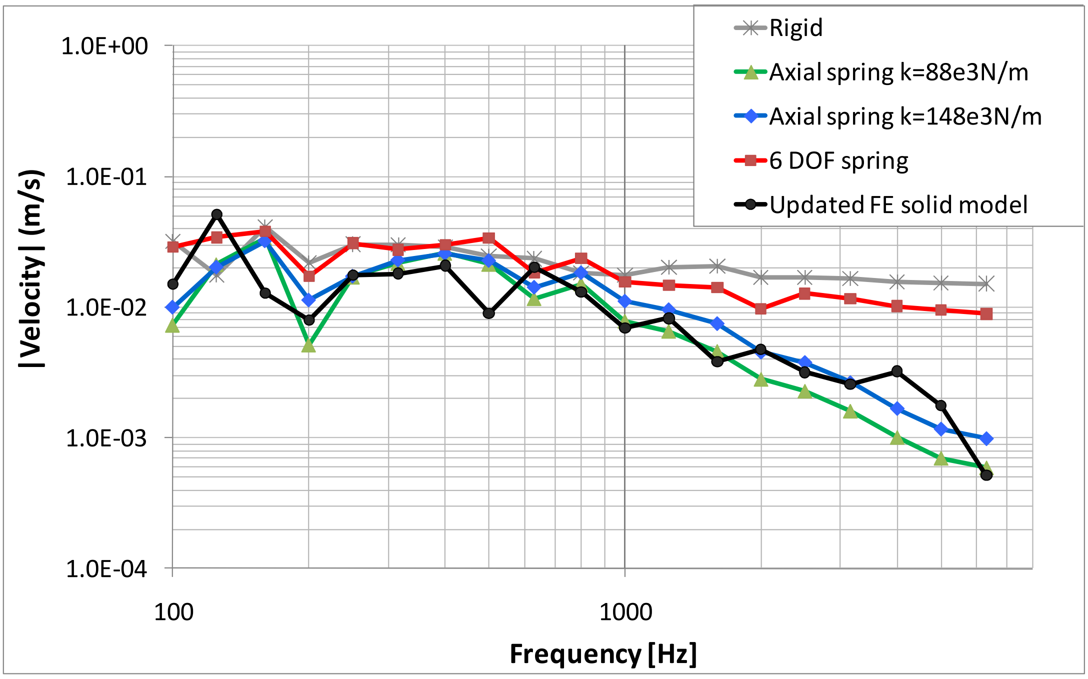

Figure 7. Upper plate velocity average in 1/3 octave frequency band,

Based on Fig. 7, in the middle frequency range, i.e. frequencies from 100 to 1000 Hz, it can be verified that all models have similar behavior, with the updated FE model presenting lower vibration most of this frequency range. In the high frequency range, i.e. frequencies above 1000 Hz, it can be observed:

- axial spring models also present lower vibration levels;
- rigid link and the 6 DOF spring model follow similar trend and reach the highest levels;
- updated FE model in the high frequency shows velocity decrease with frequency similar to axial spring models; however, with higher vibration levels.

Based on the different isolator model approaches, it is noticeable the simple springs show responses comparable to the FE model taking into account the proper frequency range. In the high frequency range, the axial spring with constant dynamic stiffness shows the same trend and values comparable to the FE model response. However for the 4000 Hz frequency band there is a vibration increase which can be associated to the isolator internal resonances and can overestimate the isolator attenuation.

Furthermore, an additional drawback to evaluate these high frequency results, it is related to the FEM feature. The responses are deterministic and taken at specific point, which insert influence of plate local modes. In the current case, although the results were averaged in order to minimize this effect, this influence can affect the results interpretation. An alternative to overcome this issue and make easier the comparison between models could consider energy parameters, such as spectral density applied in the random analysis, or averaged energy parameters in the statistical energy analysis (SEA) approach. Moreover, this current work is interested in vibration transmission from fuselage to interior panels and the consequent noise radiation, which can be significant until 10 kHz. Thus, the high frequency range is of great relevance and concern.

5. TRANSMISSION PATH ANALYSIS VIA SEA

As presented in the previous section, simplified models are not feasible for predicting the high frequency vibration transmission through an isolator. In this frequency range, although FEA can be employed, its results bring a complex task in interpreting the influence of isolator modes, due to the plate high modal density.

At the same time, in order to obtain the response of complex structures, coupled through isolators, the use of FEM can be cost prohibited due to the high level of discretization required for the high frequency range. As an alternative, for vibroacoustic problems in this frequency range, SEA is largely used, including in the aerospace industry (Lyon and DeJong, 1995).

Hence, in order to clarify the relevance of considering the isolator resonances, it is required to assess the importance of the structure-borne path at high frequency. This is performed through SEA. In this analysis the isolator is represented by a coupling loss factor (CLF), which is a measure of the rate of energy flowing through a coupling from one subsystem to another subsystem (Lyon and DeJong, 1995). The isolator is represented by CLF since so far there is no SEA subsystem formulation for isolators. In addition, the isolator has a localized effect, which restrains the proper calculation of statistical parameters required for a SEA subsystem.

A SEA model was created considering isolated plates attached at the four corners and spaced 80 mm. The analyses consider two distinct connections; the plates are connected first by a rigid link and after by a spring with the dynamic stiffness given by Tab. 3. The different connection results are also compared to the disconnected case. The analysis was performed using the commercial software VaOne (ESI Group, 2009)

A power input W_{in} of 1 W is injected in the bottom plate. The airborne and structure-borne paths are analyzed, by considering an air cavity between plates. For comparison purposes absorption material are included into the cavity. Then, the acoustic power radiated by the upper plate W_{out} is calculated. Based on this data, the response is shown as sound transmission loss TL in decibels dB, which is defined by the Eq. (4):

$$TL = 10\log\left(\frac{W_{in}}{W_{out}}\right) \quad (4)$$

In this case the higher the TL the higher the noise attenuation.

Figure 8(a) shows the comparison between the different connections when only the structure borne path is taken into account. It is noticeable that the isolator modeled as spring reduced the transmission energy in high frequency starting at 2000 Hz; the same behavior appears in upper plate velocity. Figure 8(b) demonstrates this attenuation is independent of the air cavity modeling. On the other hand, the air cavity attenuates the noise at frequencies below 1000 Hz. However, it does not affect the plate velocity, which indicates the vibration is only generated by the structural path.

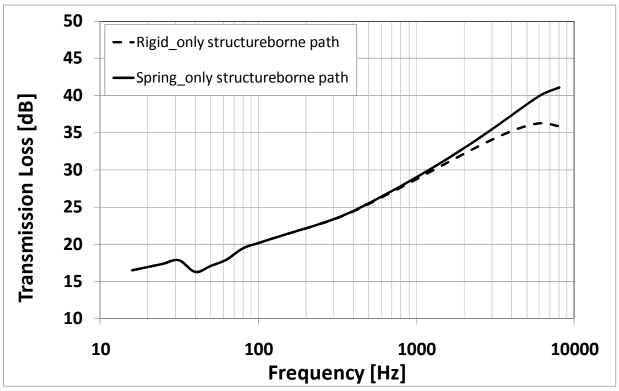

a. Only structure borne path considered

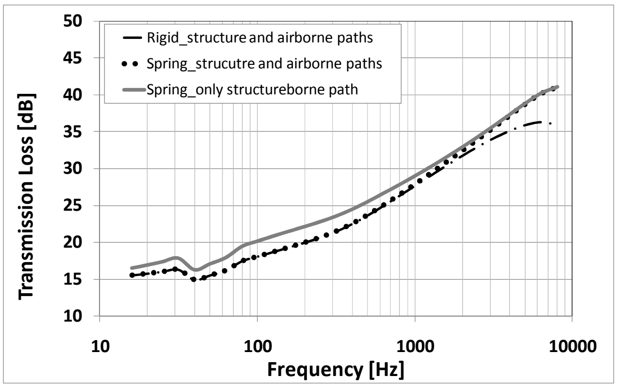

b. Structure and airborne path considered

Figure 8. Comparison between isolator and rigid connection.

Figure 9(a) shows the maximum isolator attenuation performance which can be achieved in this system in the frequency above 2000 Hz by disconnecting the plates. Besides the high frequency reduction, the elimination of the structural path reduces also the energy transmission below 1000 Hz, which shows that even though the structural path is a important contributor, it is not depend on the isolator presence, i.e. the isolator only makes real difference in the TL at high frequency.

Additionally, Fig. 9(b) shows TL is increased from frequencies below 1250 Hz by attenuating the airborne path with an absorption material, in this case light glass wool with 40 mm of thickness and density of 16 kg/m³. Although the treatment reduces drastically the airborne energy transmission at high frequency, the resultant TL is not affected since the structural path is dominant.

Based on the fact that the structure borne path, and consequently the isolator, is of great importance at high frequency, it is essential to model properly the isolator at this frequency range. This includes accounting for the isolator internal resonances, which tend to reduce the vibration attenuation.

An alternative to include the isolator dynamic behavior into a SEA analysis is to employ a hybrid FE-SEA method (Gardner *et al.*, 2005). This method encompasses the advantages of FEA and SEA method. It allows including details of a system or coupling through finite element method into a SEA model. Ongoing studies are being developed to apply this hybrid technique, which is already available in commercial software (VaOne, 2005), to predict the isolator performance and to compare it with the different models described in this paper.

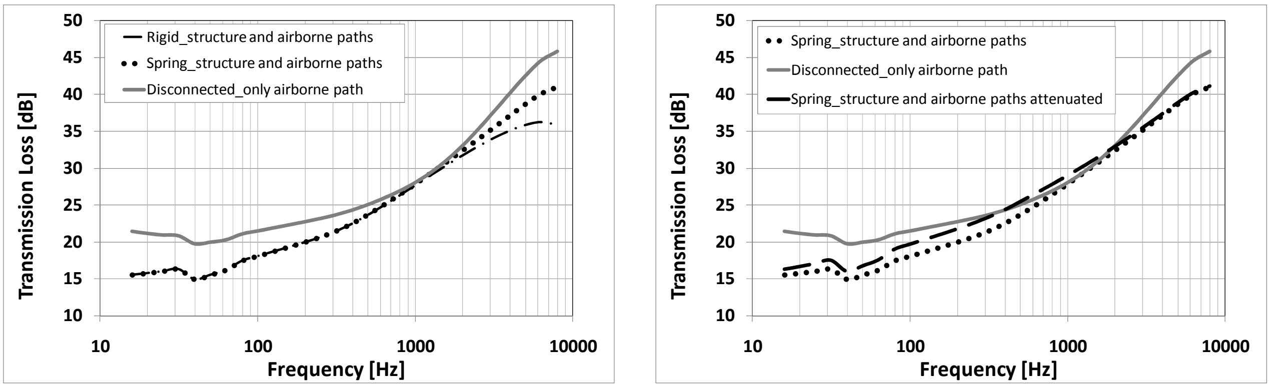

a. Structure and airborne path comparison.

b. Structure and airborne path attenuated: by isolator and absorption material, respectively

Figure 9. Comparison between isolator and rigid connection with the disconnected case.

6. CONCLUSIONS

Within this paper the FE model of a typical aeronautic isolator was developed. Based on this model was possible to identify the isolator dynamic behavior: spring modes, and the elastomeric material modes.

Different forms of modeling an isolator were applied between two plates. The comparison demonstrates that the simplified models, such as axial spring and 6 DOF spring, can be easily and well employed depending on the frequency range of interest. Although in low frequency some agreement is verified, in high frequency the simplified models can not reach a satisfactory result when compared to the isolator FE model.

On the other hand, in order to model the isolator through finite elements with fidelity, the elastomer material properties must be reliable and be available, which could be a challenger. The FE model development is time consuming, mainly due to the fine mesh required for a high frequency limit.

The high plate modal density in high frequency range caused difficulties on interpreting the isolator influence in the plate response. Although average values can be used, FEA nodal responses intricate this analysis.

For the system presented in this paper, the isolator is vital at high frequency, regardless of the air cavity modeling between plates. The structure-borne path is important in low frequency, however in this case it is not affected by the isolator. Adding an absorption material, which lessen the airborne path, TL is only increased in mid and low frequency, since in high frequency the dominant path is through the connections, i.e. through the isolator.

When the high frequency vibration transmission is a concern, such as in aircraft interior panel's noise radiation problems, a proper modeling of the isolator is required in order to considered its internal resonances. Hybrid model gathering FEM and SEA will be employed in next steps of this research in order to cover this issue.

All the discussion and results presented herein are part of ongoing research, which is aimed at developing a modeling procedure for evaluating aeronautic isolators applied in aircraft interior panels.

8. REFERENCES

Bathe, K. J., 1996, “Finite Element Procedures”, Ed. Prentice-Hall, New Jersey, USA, 1037 p.
Beranek, L. L., Vér, I. L. , 1992, “Noise and Vibration Control Engineering - Principles and Application”, Ed. Jonh Wiley & Sons Inc., New Jersey, USA, 804 p.
Clark, M. D., Hain, H. L., 1996, “A systematic approach used to design floor panel isolation for commercial aircraft”, Noise-Con 96, Seattle, USA, pp 455-460.
Downey, P., Bachman, G., and Diffendall, C., 2001, “Microcellular resilience for optimised insertion loss using an elastomeric insulating material”, Proceedings of Noise-Con 2001, Portland, USA.
ESI Group, 2009, “VaOne 2009”.
Fahy, F., Gardonio, P., 2007, “Sound and Structural Vibration”,2º Edition, Ed. Elsevier, Oxford, UK.
Gardner, B. K., Shorter, P.J., and Cotoni, V., 2005, “Modeling vibration isolators at mid and high frequency using Hybrid FE-SEA Analysis”, Proceedings of InterNoise2005, Rio de Janeiro, Brazil.
Jones, D. I. G., 2001, “Handbook of Viscoelastic Vibration Damping”, Ed. Jonh Wiley & Sons Inc., West Sussex England, 391 p.
Lyon, R. H., DeJong, R. G., 1995, “Theory and Application of Statistical Energy Analysis”, Ed. Butterworth-Heinemann, Boston, EUA, 277 p.

Lord Corporation, 6 June 2010, <http://www.lord.com>.

Material Data Base, , 6 June 2010. <http:// www.matbase.com >.

Molloy, C. T., 1957, "Use of Four-Pole Parameters in Vibration Calculations", Journal of the Acoustical Society of America, 29 (7), 842-853.

MSC Software, 2008, "MSC Nastran 2008 Quick Reference Guide".

Nashif, A.D., Jones, D.I, Henderson, J.P., 1985, "Vibration Damping", Ed. John Wiley & Sons Inc., New York, USA.

Snowdon, J. C., 1979, "Vibration Isolation: Use and Characterization", Journal of the Acoustical Society of America, 66 (5), 1245-1274.

Weisbeck, J. N., 2006, "Effect of stiffness, damping, and design on side panel isolator noise attenuation characteristics", Proceedings of InterNoise2006, Honolulu, USA.

Weisbeck, J. N., R. M. Sanetick, and T. R. L. Zmijevski, 2009, "Structure borne noise control of oscillating pumps", Proceedings of InterNoise2009, Ottawa, Canada.

5. RESPONSIBILITY NOTICE

The authors are the only responsible for the printed material included in this paper.